

This is the accepted manuscript made available via CHORUS. The article has been published as:

Probing Wilson loops in the QCD instanton vacuum

Yizhuang Liu and Ismail Zahed

Phys. Rev. D **91**, 034023 — Published 24 February 2015

DOI: [10.1103/PhysRevD.91.034023](https://doi.org/10.1103/PhysRevD.91.034023)

Probing Wilson Loops in the QCD Instanton Vacuum

Yizhuang Liu* and Ismail Zahed†

Department of Physics and Astronomy, Stony Brook University, Stony Brook, New York 11794-3800, USA

We discuss the quark and gluon condensates in the presence of a rectangular Wilson loop using the QCD instanton vacuum with three light dynamical quarks. The scalar quark condensate is found to decrease while the gluon condensate to increase. We also derive the static potential between two QCD dipoles and show that it is attractive but short ranged at large distances. Its relevance to static QCD string interactions is discussed.

PACS numbers:

I. INTRODUCTION

QCD is the fundamental theory of strong interactions. It has proven challenging in the infrared as its fundamental constituents are confined. In this regime, the quarks and gluons interact strongly and form strongly interacting hadrons. The instanton approach to the QCD vacuum allows for a semi-classical description of the QCD vacuum that is well supported by lattice simulations [1–3] (and references therein). It captures the essentials of the spontaneous breaking of chiral symmetry, accounts for the breaking of conformal symmetry and provides a mechanism for a large mass for the pseudo-scalar singlet through mixing with the fluctuations in the topological charge.

The instanton approach to the Yang-Mills vacuum does not provide a mechanism for confinement. However, in the presence of light quarks the QCD string breaks asymptotically owing to screening by the fundamental charges. In the presence of light quarks a large Wilson loop traced by a heavy quark pair at a separation a is screened by the formation of a pair of heavy-light mesons as shown in Fig. 1 (right). Interactions of light-light and heavy-light quarks can be addressed simultaneously in the QCD instanton vacuum [4, 5].

Several lattice simulations have shown that the scalar quark condensate depletes near a heavy quark sourced by a Polyakov line [6] or a static quark-antiquark string spanned by a Wilson line [7]. The squared topological density was also found to decrease near a heavy quark source [8]. In this paper we probe the quark and gluon clouds around a small and large Wilson loop in the QCD instanton vacuum with heavy and light quarks. Many of our results are amenable to a quantitative comparison with QCD lattice simulations in the unquenched approximation using Wilson loops.

In section 2 we briefly review the salient features of the QCD instanton vacuum and summarize the relevant quark and gluon correlations. The effective interactions between light and heavy quarks are also briefly discussed.

In section 3 we analyze the scalar condensates around a small Wilson loop in the one-instanton approximation. In section 4 we derive explicit relations for the scalar, pseudo-scalar quark and gluon condensates in the presence of a large Wilson loop in the screened QCD instanton vacuum. In section 5 we discuss the dominant contributions to the static dipole-dipole interaction both for small and large dipole sizes. Our conclusions are in section 6.

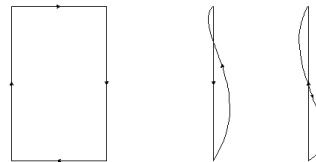


FIG. 1: Large Wilson loop: unscreened in YM (left) and screened in QCD (right). See text.

II. QCD INSTANTON VACUUM

Throughout this section we will follow the notations and the results of the general N_f bosonization scheme developed in [9]. The original $N_f = 2$ bosonization scheme was developed by Diakonov and Petrov and is summarized in [2]. The reader interested in more details regarding the derivations should consult these two references for completeness. Throughout, we will use Euclidean notations unless specified otherwise.

*Electronic address: yizhuang.liu@stonybrook.edu

†Electronic address: ismail.zahed@stonybrook.edu

A. Light Quarks

One of the key aspect of the QCD instanton vacuum is that light quarks acquire a momentum dependent constituent quark mass by rescattering through randomly distributed instanton and anti-instanton configurations. Specifically and for massless light quarks [2, 9]

$$S(x) = \langle T^* q(x) q^\dagger(0) \rangle = \int \frac{d^4 k}{(2\pi)^4} \frac{e^{ik \cdot x}}{\gamma \cdot p - iM(k)} \quad (1)$$

with the momentum dependent constituent quark mass

$$M(k) = \frac{\lambda n}{N_c} k^2 \left(\pi \bar{\rho}^2 \frac{d}{dx} (I_0 K_0 - I_1 K_1) \right)^2 \quad (2)$$

where $x = k\bar{\rho}/2$. Note that the quark zero mode is expressed in terms of Bessel functions in Fourier space. The instanton density fixes the gluon condensate in the QCD instanton vacuum $\langle F^2 \rangle = 32\pi^2 n$. The inverse mass parameter $\lambda \approx 0.34 \text{ fm}$ follows by self-consistency. Typically $n \approx 1/\text{fm}^4$ and $\bar{\rho} \approx 1/3 \text{ fm}$. As a result, the vacuum breaks spontaneously chiral symmetry and develops a chiral condensate. For a single flavor species

$$\langle \bar{q}q \rangle = -4N_c \int \frac{d^4 k}{(2\pi)^4} \frac{M(k)}{k^2 + M(k)^2} \quad (3)$$

with $\bar{q} \equiv (iq)^\dagger$ the quark field in Minkowski space. Throughout the Euclidean notation will be used unless specified otherwise. A good approximation to $S(x)$ at large $|x|$ follows from using $M_0 = M(k \approx 0) \approx 300 - 400 \text{ MeV}$, with

$$S(x) \approx \frac{iM_0^2}{4\pi^2} \left(\frac{\gamma \cdot x}{x^2} K_2(M_0 x) + \frac{1}{x} K_1(M_0 x) \right) \quad (4)$$

Typical scalar quark correlations in the QCD instanton vacuum are captured by

$$C(x) \equiv \langle T^* q^\dagger q(x) q^\dagger q(0) \rangle = C^0(x) + C^1(x) \quad (5)$$

where the first term is the connected contribution in Fig.1 (left)

$$C^0(x) = \text{Tr} |\gamma_5 S(x)|^2 \quad (6)$$

which is dominant for small $|x|$. The second contribution stems from the disconnected contribution of Fig.1 (right). In the mean-field approximation its Fourier transform is [2, 9]

$$C^1(p) = 2N_c \frac{R^2(p)}{\Delta_+(p)} \quad (7)$$

For small 4-momentum

$$\Delta_+(p) = \frac{f_+^2}{4N_c} (M_+^2 + p^2 + \mathcal{O}(m^2, p^4)) \quad (8)$$

For $N_f = 3$ light flavor masses $m = 5 \text{ MeV}$: $f_\sigma \equiv f_+ = 110 \text{ MeV}$ and $m_\sigma \equiv M_+ = 640 \text{ MeV}$. This exchanged meson is identified with the light scalar meson with $m_\sigma \equiv M_+ < 2M_0$, below the $q\bar{q}$ threshold. The residue at the pole is [2, 9]

$$R(0) = \int \frac{d^4 k}{(2\pi)^2} \frac{2}{M(k)} \frac{k^2/M(k)^2 - 1}{(1 + k^2/M(k)^2)^2} \quad (9)$$

so that

$$C^1(x) \approx \frac{4N_c^2 R^2(0)}{f_\sigma^2} \frac{m_\sigma}{4\pi^2 |x|} K_1(m_\sigma |x|) \quad (10)$$

which is dominant for large $|x|$.



FIG. 2: Meson correlator: connected (left) and disconnected (right). See text.

The pseudo-scalar correlator follows from similar arguments with

$$C_5(x) \equiv \langle T^* q^\dagger \gamma_5 q(x) q^\dagger \gamma_5 q(0) \rangle = C_5^0(x) + C_5^1(x) \quad (11)$$

with the connected part

$$C_5^0(x) = \text{Tr} |S(x)|^2 \quad (12)$$

and the disconnected part [2, 9]

$$C_5^1(p) = N_c \frac{R_5^2(p)}{\Delta_-(p) + 3\chi_*/2N_c} \quad (13)$$

Here $\chi_\star = n \approx 1/\text{fm}^4$ is the quenched topological susceptibility, and

$$R_5(0) = -2 \int \frac{d^4 k}{(2\pi)^2} \frac{M(k)}{M(k)^2 + k^2} \quad (14)$$

Again, for small 4-momentum

$$\Delta_-(p) = \frac{f_-^2}{4N_c} (M_-^2 + p^2 + \mathcal{O}(m^2, p^4)) \quad (15)$$

For $N_f = 3$ light flavor masses $m = 5$ MeV: $f_\pi \equiv f_- = 88$ MeV and $m_\pi \equiv M_- = 160$ MeV, are the pseudo-scalar decay constant and mass respectively. $m_\pi \equiv M_-$ obeys the GOR relation [10] and vanishes in the chiral limit.

(14) captures the soft pion theorem for the pseudoscalar coupling to a constituent quark with fixed flavor $g_\pi \equiv \langle \bar{q}q \rangle / f_\pi = 2N_c R_5(0) / f_\pi$, in terms of which (13) reads

$$C_5^1(p) \approx \frac{g_\pi^2}{p^2 + m_\pi^2 + 2N_f \chi_\star / f_\pi^2} \quad (16)$$

which exhibits explicitly the η' pole with $m_{\eta'}^2 = m_\pi^2 + 2N_f \chi_\star / f_\pi^2$. Typically $\langle \bar{q}q \rangle \approx (-271 \text{ MeV})^3$ from the GOR relation with the pion parameters quoted, so that $g_\pi^2 \approx (475 \text{ MeV})^4$ and $m_{\eta'} \approx 1125$ MeV. Similarly, we may identify the scalar coupling to a constituent quark of fixed flavor as $g_\sigma = 2\sqrt{2}N_c R(0) / f_\sigma$, in terms of which (7) takes the canonical form

$$C^1(p) \approx \frac{g_\sigma^2}{p^2 + m_\sigma^2} \quad (17)$$

with the σ pole explicit. Chiral symmetry implies $g_\pi \approx g_\sigma$ between the scalar and pseudo-scalar coupling.

B. Gluons

The gluonic correlations in the QCD instanton vacuum mix with the fermionic correlations as shown in Fig.3. Throughout we will define $\text{Tr}(gF)^2 \equiv F^2$ unless noted otherwise. With this in mind, the scalar gluon correlation function is [9]

$$\langle T^* F^2(x) F^2(0) \rangle_c = \int \frac{d^4 p}{(2\pi)^4} e^{ip \cdot x} \left(\frac{1}{\sigma_\star^2} - \frac{N_f}{2N_c \Delta_+(p)} \right)^{-1} \quad (18)$$

The ultra-local contribution is the is the quenched gluon compressibility $\sigma_\star^2 = 12n/11N_c \approx 0.36/\text{fm}^4$. Thus

$$\langle T^* F^2(x) F^2(0) \rangle_c = \sigma_\star^2 \delta^4(x) + \frac{N_f \sigma_\star^4}{f_\sigma^2} \frac{m_s}{2\pi^2 |x|} K_1(m_s |x|) \quad (19)$$

with $m_s^2 = m_\sigma^2 - 2N_f \sigma_\star^2 / f_\sigma^2$ which is lighter than m_σ due to the fluctuations in the instanton density as captured by the quenched gluon compressibility. For the typical vacuum parameters quoted earlier, $m_s \approx 349$ MeV which is in the range of the constituent quark mass $M_0 \approx 300 - 400$ MeV and below the sigma meson $m_\sigma \approx 640$ MeV.



FIG. 3: Gluon correlator: connected and ultra-local (left) and disconnected (right). See text.

The pseudo-scalar gluon correlation function [2, 9]

$$\langle T^* F \tilde{F}(x) F \tilde{F}(0) \rangle = \int \frac{d^4 p}{(2\pi)^4} e^{ip \cdot x} \left(\frac{1}{\chi_\star} + \frac{N_f}{2N_c \Delta_-(p)} \right)^{-1} \quad (20)$$

simplifies to

$$\langle T^* F \tilde{F}(x) F \tilde{F}(0) \rangle = \chi_\star \delta^4(x) - \frac{N_f \chi_\star^2}{f_\pi^2} \frac{m_{\eta'}}{2\pi^2 |x|} K_1(m_{\eta'} |x|) \quad (21)$$

We note that in the quenched approximation ($N_f = 0$) both the scalar and pseudo-scalar glueballs are infinitely heavy in leading order in the QCD instanton vacuum. The fluctuations in the instanton and anti-instanton numbers cause the scalar and pseudo-scalar glueballs to be lighter through mixing. Specifically: $m_s \approx m_\sigma - N_f / N_c^2$ (scalar glueball) and $m_{ps} \equiv m_{\eta'} \approx m_\pi + N_f / N_c$ (pseudo-scalar glueball). The $1/N_c$ shifts are sub-leading but tied to the QCD anomalies: the former to the scale anomaly and the latter to the U(1) axial anomaly. Overall, they maybe affected by higher order and non-anomalous $1/N_c$ corrections neglected in the bosonization analysis in [9].

C. Heavy and Light Quarks

In the instanton vacuum heavy and light quarks interact. The effective vertices for heavy-light interactions were discussed in [4, 5]. For 2 light flavors in the presence of a heavy quark Q , the induced interaction is typically of the form [4, 5]

$$\mathcal{L}_{qqQ} \approx -i\kappa_{qqQ} Q^\dagger \frac{(1+i\gamma^4)}{2} Q \left(\det q_L^\dagger q_R + \det q_R^\dagger q_L \right) \quad (22)$$

A Fierz rearrangement of (22) reads

$$\begin{aligned} & -i\kappa_{qqQ} Q^\dagger \frac{(1+i\gamma^4)}{8} Q \\ & \times (u^\dagger u d^\dagger d + u^\dagger \gamma_5 u d^\dagger \gamma_5 d + u^\dagger \gamma^{\nu\mu} u d^\dagger \gamma^{\nu\mu} d) \end{aligned} \quad (23)$$

which will be used below. (22) is to be compared to the standard t' Hooft interaction [11]

$$\mathcal{L}_{qqq} \approx i\kappa_{qqq} \left(\det q_L^\dagger q_R + \det q_R^\dagger q_L \right) \quad (24)$$

for $N_f = 3$ light flavors. Typically: $\kappa_{qqQ}/\kappa_{qqq} \approx 0.08$ [4]. For the parameters of the QCD instanton vacuum $\kappa_{qqQ} \approx 0.012 \text{ fm}^5$ with a constituent quark mass $M_0 \approx 400 \text{ MeV}$. The interaction (22) induces bound scalar, pseudo-scalar and tensor states with a typical size at the origin [5]

$$|\phi_{qQ}(0)|^2 \equiv \frac{1}{a_{qQ}^3} \approx \left(\frac{2\pi^2 f_{qQ}^2}{N_c} \right)^{3/2} \quad (25)$$

For a D-meson $f_D \leq 290 \text{ MeV}$ so that $a_{qQ} \approx 0.26 \text{ fm}$.

III. SMALL WILSON LOOP IN THE ONE-INSTANTON APPROXIMATION

We first assess the effects of a single instanton and anti-instanton on a small Wilson loop of size a . The case of a large Wilson loop in the presence of many instantons and anti-instantons will be considered next. To estimate the scalar condensate near the center x of the Wilson-loop we use the OPE expansion in the form

$$\frac{W}{\langle W \rangle} = 1 - \frac{2a^4 \pi^2}{N_c} F^2(x) + \mathcal{O}(a^6) \quad (26)$$

The leading operator contribution to the scalar condensate in a Wilson-loop follows from the mixed operator $\langle q^\dagger q F^2 \rangle$. In the one-instanton approximation and for arbitrary flavors N_f

$$\langle q^\dagger q(x) F^2(x) \rangle \approx \frac{384 N_f}{\pi^2} \int \frac{d\mu_{B+F}}{im} \frac{\rho^6}{(|x-x_o|^2 + \rho^2)^4} \quad (27)$$

with the one-loop density [12]

$$\begin{aligned} \frac{d\mu_{B+F}}{d^4 x_0 d\rho} &= \frac{2^{4N+2} \pi^{4N-2}}{(N-1)!(N-2)! \pi^{2(N_f-1)}} \frac{1}{\pi^{2(N_f-1)}} \\ &\times \left(\frac{\rho M_{PV}}{g} \right)^{4N} \left(\frac{m}{M_{PV}} \right)^{N_f} e^{-\frac{8\pi^2}{g^2}} \end{aligned} \quad (28)$$

with M_{PV} a Pauli-Villars UV regulator. The quark condensate in the one-instanton approximation is

$$\langle q^\dagger q(x) \rangle \approx \frac{4N_f}{\pi^2} \int \frac{d\mu_{B+F}}{im} \frac{\rho^2}{(|x-x_o|^2 + \rho^2)^3} \quad (29)$$

Thus

$$\frac{\langle q^\dagger q(x) W \rangle_c}{\langle q^\dagger q \rangle \langle W \rangle} \approx -\frac{64\pi^2 a^4}{5N_c \bar{\rho}^4} \quad (30)$$

where we have fixed $\rho \approx \bar{\rho}$ in the instanton density.

The scalar gluonic cloud in a small Wilson loop in the one-instanton approximation follows a similar reasoning with

$$\langle F^2(x) F^2(x) \rangle \approx \frac{(192)^2}{\pi^2} \int d\mu_{B+F} \frac{\rho^8}{(|x-x_o|^2 + \rho^2)^8} \quad (31)$$

so that

$$\frac{\langle F^2(x) W \rangle_c}{\langle F^2 \rangle \langle W \rangle} \approx -\frac{384\pi^2 a^4}{7N_c \bar{\rho}^4} \quad (32)$$

Since $\langle F \tilde{F} F^2 \rangle = \langle q^\dagger \gamma_5 q F^2 \rangle = 0$ by parity, the pseudo-scalar condensates around a small Wilson loop vanish. Both the scalar quark and gluon condensates decrease near a small Wilson loop in the one-instanton approximation.

IV. LARGE WILSON LOOP IN THE QCD INSTANTON VACUUM

The QCD instanton vacuum involves an ensemble of instantons and anti-instantons. In this case, the one loop density (28) is substituted by its mean value for the average instanton size [13]

$$\frac{d\mu_{B+F}}{d^4 x d\rho} \rightarrow n \delta(\rho - \bar{\rho}) \quad (33)$$

In particular, the one-instanton zero mode in (29) turns to a quasi-zero mode with $im \rightarrow \lambda + im$ with a semi-circular spectral distribution $\nu(\lambda)$ (normalized to 1) so that

$$\langle q^\dagger q \rangle = n \int \frac{\nu(\lambda) d\lambda}{\lambda + im} \rightarrow -i\pi n \nu(0) \quad (34)$$

in the chiral limit. (32) is the Banks-Casher relation [14] between the spectral density and the chiral condensate in the QCD instanton vacuum. Note that in Euclidean space, the chiral condensate is purely imaginary with the convention $\bar{q} = (iq)^\dagger$.

Large Wilson loops in the QCD vacuum are screened by light quarks as shown in Fig. 1. The Wilson loop as a correlator $\langle Q^\dagger(a)Q(0) \rangle$ can be thought as a heavy-light meson correlator $\langle Q^\dagger \gamma q(a) q^\dagger \gamma Q(0) \rangle$ after screening with $\gamma = (1, \gamma_5)$. We recall that the pseudo-scalar B -meson ($\gamma = \gamma_5$) is degenerate with the scalar D -meson ($\gamma = 1$) by unbroken chiral symmetry. Each of the two mesons are part of two heavy-light multiplets which are degenerate by heavy-quark symmetry, i.e. $(B, B^*) = (0^-, 1^-)$ and $(D, D^*) = (0^+, 1^+)$ respectively. Broken chiral symmetry shifts slightly down (B, B^*) and up (D, D^*) [15–18]. In this section, we will analyze both the fermionic and gluonic condensates in a large Wilson loop screened by light quarks using the QCD instanton vacuum.

A. Scalar Quark Condensate

A measure of the scalar condensate in the large Wilson loop of Fig.1 (right) amounts to the contributions shown in Fig. 4. The screened Wilson lines in QCD are tied to the condensate insertion (black blob) through a pair of re-scattering quarks in the QCD vacuum. The gray blobs are the heavy-light Qqq effective vertices. The contribution on the left is of order κ_{qqQ} while that on the right is of order κ_{qqQ}^2 and sub-leading. The leading contribution is $(x_W = (\tau, \mathbf{0}))$

$$\frac{\langle q^\dagger q(x)W \rangle_c}{\langle W \rangle} = 2i \frac{\kappa_{qqQ}}{a_{qQ}^3} \int d\tau \langle T^* q^\dagger q(x_W) q^\dagger q(x) \rangle \quad (35)$$

The factor of 2 is due to the two possible insertions on the screened heavy quarks.

From (5) it follows that

$$\frac{\langle q^\dagger q(x)W \rangle_c}{\langle W \rangle} \approx 2i \frac{\kappa_{qqQ}}{a_{qQ}^3} (C^0(L) + C^1(L)) \quad (36)$$

with the probing point at $x = (x_4, L)$. Because of x_4 -translational invariance, (36) depends only on the spatial distance L . The purely imaginary nature of the result in Euclidean space is due to the zero modes. Using (34) we can re-write (36) in real form in Minkowski space as

$$\frac{\langle \bar{q}q(x)W \rangle_c}{\langle \bar{q}q \rangle \langle W \rangle} \approx -\frac{2\kappa_{qqQ}}{a_{qQ}^3 \pi n\nu(0)} (C^0(L) + C^1(L)) \quad (37)$$

The connected contribution to the scalar quark correlator is

$$C^0(L) = \frac{M_0^4 N_c}{4\pi^4} \int d\tau \frac{K_2(M_0 \sqrt{L^2 + \tau^2})^2 - K_1(M_0 \sqrt{L^2 + \tau^2})^2}{L^2 + \tau^2} \quad (38)$$

and asymptotes

$$C^0(L) \approx \frac{3N_c M_0^5}{8\pi^3} \frac{e^{-2M_0 L}}{(M_0 L)^3} \quad (39)$$

after using the expansion

$$K_\alpha(x) = \sqrt{\frac{\pi}{2x}} e^{-x} \left(1 + \frac{2\alpha^2 - 1}{8x} + \dots\right) \quad (40)$$

The disconnected contribution follows similarly

$$C^1(L) \approx \frac{g_\sigma^2 m_\sigma}{\sqrt{32\pi^3}} \frac{e^{-m_\sigma L}}{\sqrt{m_\sigma L}} \quad (41)$$

Both (39) and (41) are positive making the result (37) negative. The scalar quark condensate depletes near a large Wilson loop in overall agreement with the lattice results [6, 7]

B. Pseudo-scalar Quark Condensate

The pseudo-scalar condensate in a large and screened Wilson loop can be sought by similar arguments. However, we note that the leading contribution of order κ_{qqQ} as shown in Fig. 4 (left) involves the Fierz pseudo-scalar vertex $u^\dagger \gamma_5 u d^\dagger \gamma_5 d$ from (22). Let $Q^\dagger \gamma u$ be a pair of heavy-light chiral partners with $\gamma = (1, \gamma_5)$. The induced vertex is

$$\langle 0 | u^\dagger \tilde{\gamma} Q [Q^\dagger (1 + i\gamma_4) Q u^\dagger \gamma_5 u] Q^\dagger \gamma u | 0 \rangle \otimes d^\dagger \gamma_5 d \quad (42)$$

For $\tilde{\gamma} = \gamma$ (42) vanishes by spin tracing. However, for nearly degenerate chiral partners by heavy quark symmetry [15, 16], the transition vertex (42) with $\tilde{\gamma} = (\gamma_5, 1)$ does not vanish. A rerun of the arguments for the scalar condensate gives

$$\frac{\langle q^\dagger \gamma_5 q(x)W \rangle_c}{\langle W \rangle} = 2i \frac{\kappa_{qqQ}}{a_{qQ}^3} \int d\tau \langle T^* q^\dagger \gamma_5 q(x_W) q^\dagger \gamma_5 q(x) \rangle \quad (43)$$

From (11) it follows that

$$\frac{\langle \bar{q} \gamma_5 q(x)W \rangle_c}{\langle W \rangle} \approx -2 \frac{\kappa_{qqQ}}{a_{qQ}^3} (C_5^0(L) + C_5^1(L)) \quad (44)$$

after translation to Minkowski space with $\gamma_5^E = -i\gamma_5^M$ and $\bar{q} = (iq)^\dagger$. The connected and disconnected contributions to the pseudo-scalar quark correlator are respectively,

$$C_5^0(L) = \frac{1}{3} C^0(L) \quad (45)$$

and

$$C_5^1(L) \approx \frac{g_\pi^2 m_{\eta'}}{\sqrt{8\pi^3}} \frac{e^{-m_{\eta'} L}}{\sqrt{m_{\eta'} L}} \quad (46)$$

which is to be compared to (41).

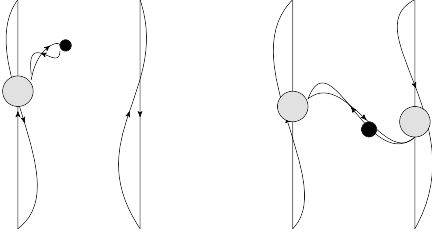


FIG. 4: Screened large Wilson loop of width a with a condensate insertion (black blob). See text.

C. Scalar Gluon Condensate

The gluon condensate surrounding a large Wilson loop follows similar arguments. First, we note that the screened $Q^\dagger q$ state acts as a colored electric dipole of size a_{qQ} sourcing a composite Coulomb field. An estimate of the pertinent electric vertex follows from second order perturbation theory [19, 20]

$$\frac{|\langle 0|(a_{qQ} E^a)|1\rangle|^2}{(g^2/a_{qQ})} \approx (a_{qQ}^3/g^2) E^a E^a \quad (47)$$

where the perturbative Coulomb splitting between the singlet and octet state was used. This approximation is valid as long as the perturbative Coulomb potential is greater than the instanton Coulomb potential in the bound state or $g/a_{qQ} \gg 1/g\bar{\rho}$. In the converse, then $g^2/a_{qQ} \rightarrow 1/\bar{\rho}$ so that

$$\frac{|\langle 0|(a_{qQ} E^a)|1\rangle|^2}{(1/\bar{\rho})} \approx (a_{qQ}^2 \bar{\rho}) E^a E^a \quad (48)$$

For our problem $a_{qQ} \approx \bar{\rho} \approx 1/3$ fm and $g \equiv g(\bar{\rho}) \approx 2$ making (47) more appropriate for the screened Wilson loop.

With this in mind, a rerun of the preceding arguments give

$$\frac{\langle F^2(x)W \rangle_c}{\langle W \rangle} = +2 \frac{a_{qQ}^3}{g^2} \int d\tau \frac{1}{2} \langle T^* F^2(x_W) F^2(x) \rangle \quad (49)$$

Instantons carry $E = B$ in Euclidean space by self-duality, i.e. $E^2 \equiv F^2/2$. So the gluonic insertion measures the amount of gluonic correlations

$$\frac{\langle F^2(x)W \rangle_c}{\langle W \rangle} = \frac{a_{qQ}^3}{g^2} \frac{N_f \sigma_*^4 m_s}{2\pi^2 f_\sigma^2} \int d\tau \frac{K_1(m_s \sqrt{L^2 + \tau^2})}{\sqrt{L^2 + \tau^2}} \quad (50)$$

For large L ,

$$\frac{\langle F^2(x)W \rangle_c}{\langle F^2 \rangle \langle W \rangle} \approx + \frac{N_f}{64\pi^2} \frac{a_{qQ}^3 \sigma_*^4 m_s}{g^2 n f_\sigma^2} \frac{e^{-m_s L}}{\sqrt{2\pi^3 m_s L}} \quad (51)$$

after using $\langle F^2 \rangle = 32\pi^2 n$. The gluon condensate is enhanced near a large Wilson loop.

D. Pseudo-scalar Gluon Condensate

The pseudo-scalar gluon condensate involves the transition vertex discussed in (42) for nearly degenerate chiral heavy-light states, and mixes $F\tilde{F}$ with $q^\dagger \gamma_5 q$. Specifically,

$$\frac{\langle F\tilde{F}(x)W \rangle_c}{\langle W \rangle} = 2i \frac{\kappa_{qqQ}}{a_{qQ}^3} \int d\tau \langle T^* q^\dagger \gamma_5 q(x_W) F\tilde{F}(x) \rangle \quad (52)$$

which can be reduced using

$$\langle T^* q^\dagger \gamma_5 q(x) F\tilde{F}(0) \rangle = -4i \frac{g_\pi \chi_* m_{\eta'}}{N_c f_\pi^2} \frac{K_1(m_{\eta'} |x|)}{|x|} \quad (53)$$

Setting $x = (x_4, L)$ and using x_4 -translational invariance we obtain

$$\frac{\langle F\tilde{F}(x)W \rangle_c}{\langle W \rangle} = + \frac{\kappa_{qqQ}}{a_{qQ}^3} \frac{2\pi g_\pi}{N_c} \frac{\chi_* m_{\eta'}}{f_\pi^2} \frac{e^{-m_{\eta'} L}}{\sqrt{\pi m_{\eta'} L}} \quad (54)$$

Since $g_\pi \equiv \langle \bar{q}q \rangle / f_\pi < 0$, we conclude that the topological density decreases near a large Wilson loop.

E. Squared Scalar and Pseudo-scalar Gluon Condensates

The squared scalar and pseudo-scalar gluon condensates around a fixed and large Wilson loop can also be analyzed using similar arguments. The squared pseudo-scalar condensate reads

$$\frac{\langle (F\tilde{F}(x))^2 W \rangle_c}{\langle W \rangle} = 2i \frac{\kappa_{qqQ}}{a_{qQ}^3} \int d\tau \langle T^* q^\dagger q(x_W) (F\tilde{F})^2(x) \rangle \quad (55)$$

The correlation function in (55) can be obtained by extending the analysis in [9]. The result is

$$\langle T^* q^\dagger q(x) (F\tilde{F})^2(0) \rangle = 2i\mathcal{B} \left(\frac{16\chi_* m_{\eta'}}{f_\pi^2} \frac{K_1(m_{\eta'}|x|)}{|x|} \right)^2 \quad (56)$$

The overall constant \mathcal{B} is set by the momentum dependent constituent mass (2)

$$\mathcal{B} = \int \frac{d^4k}{(2\pi)^4} \frac{M(k)(k^2 - M^2(k))}{(k^2 + M^2(k))^2} \quad (57)$$

which is numerically positive: $\mathcal{B} \approx (150 \text{ MeV})^3$. Thus

$$\frac{\langle (F\tilde{F}(x))^2 W \rangle_c}{\langle (F\tilde{F})^2 \rangle \langle W \rangle} \approx -\frac{\kappa_{qqQ}}{a_{qQ}^3} \frac{256\pi\mathcal{B}}{\chi_*/V_4} \frac{\chi_*^2 m_{\eta'}^3}{f_\pi^4} \left(\frac{e^{-m_{\eta'}L}}{m_{\eta'}L} \right)^2 \quad (58)$$

where the normalization

$$\langle (F\tilde{F})^2 \rangle \approx \chi_* \delta^4(0) \equiv \frac{\chi_*}{V_4}$$

following from (20) was used. (58) is overall negative, an indication that the squared topological density is slightly depleted near a large Wilson loop. In the quenched approximation the analogue of (58) was analyzed on the lattice [8] with the result that the squared topological density decreases near a static color source described by a Polyakov line.

The same reasoning for the squared gluon condensate yields

$$\frac{\langle (FF(x))^2 W \rangle_c}{\langle (FF)^2 \rangle \langle W \rangle} \approx \frac{\kappa_{qqQ}}{a_{qQ}^3} \frac{256\pi\mathcal{C}}{(32\pi^2 n)^2} \frac{\sigma_*^4 m_s^3}{f_\sigma^4} \left(\frac{e^{-m_s L}}{m_s L} \right)^2 \quad (59)$$

with the constant \mathcal{C} given by the running constituent mass (2)

$$\mathcal{C} = \int \frac{d^4k}{(2\pi)^4} \frac{M^3(k)(3k^2 - M^2(k))}{(k^2 + M^2(k))^3} \quad (60)$$

Numerically: $\mathcal{C} \approx (207 \text{ MeV})^3$, so that the squared gluon condensate is slightly enhanced near a large Wilson loop.

V. DIPOLE-DIPOLE INTERACTION IN THE QCD INSTANTON VACUUM

The dipole-dipole interaction in the QCD instanton vacuum receives contributions from the gluon-gluon correlator for $a \leq a_{qQ}$ and from scalar correlations for $a \gg a_{qQ}$ as shown in Fig. 5. They will be addressed separately below. Generically, the dipole-dipole potential follows from

$$V(L) = - \lim_{T \rightarrow +\infty} \frac{1}{T} \ln \left(\frac{\langle W(L)W(0) \rangle_c}{\langle W(L) \rangle \langle W(0) \rangle} \right) \quad (61)$$

with $W(0)$ and $W(L)$ two identical and rectangular Wilson loops of width a and infinite time-extent T , centered at 0 and L respectively. Throughout this section L refers to the spatial separation between the two dipoles. For simplicity, the dipoles have identical width and are parallel.

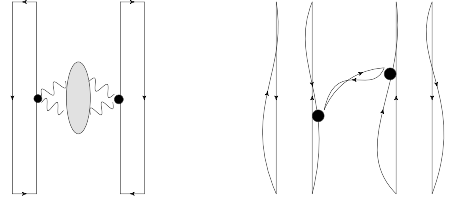


FIG. 5: Static dipole-dipole correlator: small size and un-screened dipoles (left) and large size and screened dipoles (right). See text.

A. Gluon Induced Correlations: $a \leq a_{qQ}$

For small dipole sizes $a \leq a_{qQ}$, the effects of screening can be ignored, and the dipoles source (colored) electric fields as depicted in Fig. 5 (left). As we noted earlier, the dipole sources a composite vertex $(a^3/g^2)E^2$ for $g/a > 1/g\bar{\rho}$ and $(a^2\bar{\rho})E^2$ for $g/a < 1/g\bar{\rho}$. Recall that $gE \equiv E$ in our notations. For the former

$$V_G(L) \approx -\frac{a^6}{g^4} \int d\tau \frac{1}{4} \langle T^* F^2(\tau, 0) F^2(0, L) \rangle \quad (62)$$

while for the latter $a^6/g^4 \rightarrow a^4\bar{\rho}^2$. Using the above arguments for the scalar gluon correlator in the QCD instanton vacuum we obtain (19)

$$V_G(L) = -\frac{a^6}{g^4} \frac{N_f \sigma_*^4 m_s}{8\pi^2 f_\sigma^2} \int d\tau \frac{K_1(m_s \sqrt{L^2 + \tau^2})}{\sqrt{L^2 + \tau^2}} \quad (63)$$

or asymptotically

$$V_G(L) \approx -\frac{a^6}{8g^4} \frac{N_f \sigma_*^4 m_s}{3f_\sigma^2} \frac{e^{-m_s L}}{\sqrt{2\pi^3 m_s L}} \quad (64)$$

The dipole-dipole potential is screened by the light scalar mass (19)

$$m_s = (m_\sigma^2 - 2N_f \sigma_*^2 / f_\sigma^2)^{1/2} \approx 349 \text{ MeV}$$

which is smaller than the sigma meson mass $m_\sigma \approx 640 \text{ MeV}$ due to the finite compressibility $\sigma_*^2 \approx 0.36/\text{fm}^4$ of the QCD instanton vacuum. As we noted in section IIB, the effect of the compressibility on the scalar mass m_s are of order N_f/N_c^2 .

The alternative regime with $a^6/g^4 \rightarrow a^4\bar{\rho}^2$ is to be compared to the single instanton result of $(a^4\bar{\rho}^2)/L^7$ in [19]. Non-parallel dipoles yield additional contributions to $V_G(L)$ depending on the dipoles relative orientations. They will not be discussed here.

B. Fermion Induced Correlations: $a \gg a_{qQ}$

Large size dipoles with $a \gg a_{qQ}$ are screened by the light quarks as depicted in Fig. 5 (right). They form four pairs of heavy-light bound states. Their pair interactions are then similar to the ones we discussed before, with

$$V_0(L) \approx -\frac{\kappa_{qqQ}^2}{a_{qQ}^6} \frac{3N_c M_0^5}{4\pi^3} \frac{e^{-2M_0 L}}{(M_0 L)^3} \quad (65)$$

for the connected or C^0 contribution, and

$$V_1(L) \approx -\frac{\kappa_{qqQ}^2}{a_{qQ}^6} \frac{g_\sigma^2 m_\sigma}{64} \frac{e^{-m_\sigma L}}{\sqrt{\pi^3 m_\sigma L}} \quad (66)$$

for the disconnected or C^1 contribution. All pair contributions add to the total fermionic dipole-dipole interaction

$$V_F(L) = \sum_{i=0,1} (V_i(L) + V_i(L+2a) - 2V_i(L+a)) \quad (67)$$

We also note that the leading fermionic induced interaction following by Taylor expansion

$$V_F(L) \approx a^2 \frac{\partial^2}{\partial^2 L} (V_0(L) + V_1(L)) \quad (68)$$

is also attractive. Since $m_s < m_\sigma$, the gluonic induced interaction (64) is dominant over the fermionic induced interaction (66) for dipoles of sizes $a \gg a_{qQ} \approx 0.26 \text{ fm}$.

VI. CONCLUSIONS

The QCD instanton vacuum offers a semi-classical framework for discussing quark and gluon correlations. It breaks explicitly conformal symmetry through the instanton density, and spontaneously chiral symmetry through the appearance of a chiral condensate. As a result a light pseudo-scalar flavor octet of Goldstone mesons emerge which satisfies the GOR relation. A remaining flavor singlet meson is turned heavy through the finite topological susceptibility of the QCD instanton vacuum in accordance with the U(1) axial anomaly in QCD. Scalar and pseudo-scalar gluon correlators in the QCD instanton vacuum mix with the scalar and pseudo-scalar light meson correlators.

Large Wilson loops are screened in the QCD instanton vacuum. We have explicitly analyzed the scalar and pseudo-scalar quark and gluon content of large Wilson loops and shown that they are dominated by the light scalar and pseudo-scalar meson exchanges at large distances. Because of the lack of confinement in this model, the intermediate distances are contaminated by the two constituent quark exchange as well. Recall that the latter is dominant at shorter distances.

Recently, we have analyzed similar issues in the context of AdS/QCD [20], in the double limit of a large number of colors N_c and strong 't Hooft coupling. In leading order in $1/N_c$, large Wilson loops are unscreened. In contrast, our results are derived at weak coupling for which the semi-classical of the QCD instanton vacuum is justified and fixed N_c for which screening is important since in our case $N_f/N_c = 1$. Lattice QCD simulations support the depletion of the scalar quark condensate in the vicinity of a Polyakov line [6] and a Wilson loop [7].

We have explicitly analyzed small and large static dipole-dipole interactions in the screened QCD instanton vacuum. Our analysis shows that these interactions are attractive, short ranged and dominated by the exchange of a light scalar $m_s < m_\sigma$. Owing to screening, the scalar glueballs mix in the QCD instanton vacuum, causing the static dipole-dipole interaction to deviate from the Casimir-Polder form noted in the one-instanton approximation [19].

Static dipole-dipole interactions provide a simple estimate of the static interaction between QCD strings. These interactions play an important role in addressing issues of interactions of QCD strings, in particular near the Hagedorn temperature where they may condition the

nature of the transition to a fireball as a stringy black-hole [21, 22]. We hope to address some related issues next.

VII. ACKNOWLEDGMENTS

This work was supported by the U.S. Department of Energy under Contracts No. DE-FG-88ER40388.

-
- [1] T. Schafer and E. V. Shuryak, Rev. Mod. Phys. **70**, 323 (1998) [hep-ph/9610451].
 - [2] D. Diakonov, Prog. Part. Nucl. Phys. **51**, 173 (2003) [hep-ph/0212026].
 - [3] M. A. Nowak, M. Rho and I. Zahed, Singapore, Singapore: World Scientific (1996) 528 p
 - [4] S. Chernyshev, M. A. Nowak and I. Zahed, Phys. Lett. B **350**, 238 (1995) [hep-ph/9409207].
 - [5] S. Chernyshev, M. A. Nowak and I. Zahed, Phys. Rev. D **53**, 5176 (1996) [hep-ph/9510326].
 - [6] W. Buerger, M. Faber, H. Markum and M. Muller, Phys. Rev. D **47**, 3034 (1993).
 - [7] T. Iritani, G. Cossu and S. Hashimoto, PoS Hadron **2013** (2014) 159 [arXiv:1401.4293 [hep-lat]].
 - [8] M. Faber, H. Markum, S. Olejnik and W. Sakuler, Nucl. Phys. Proc. Suppl. **34**, 167 (1994) [hep-lat/9311052].
 - [9] M. Kacir, M. Prakash and I. Zahed, Acta Phys. Polon. B **30**, 287 (1999) [hep-ph/9602314].
 - [10] M. Gell-Mann, R. J. Oakes and B. Renner, Phys. Rev. **175**, 2195 (1968).
 - [11] G. 't Hooft, Phys. Rev. D **14**, 3432 (1976) [Erratum-ibid. D **18**, 2199 (1978)].
 - [12] C. W. Bernard, Phys. Rev. D **19** (1979) 3013.
 - [13] E. V. Shuryak, Phys. Lett. B **79**, 135 (1978).
 - [14] T. Banks and A. Casher, Nucl. Phys. B **169**, 103 (1980).
 - [15] M. A. Nowak, M. Rho and I. Zahed, Acta Phys. Polon. B **35**, 2377 (2004) [hep-ph/0307102].
 - [16] W. A. Bardeen and C. T. Hill, “Chiral dynamics and heavy quark symmetry in a solvable toy field theoretic model,” Phys. Rev. D **49**, 409 (1994) [hep-ph/9304265].
 - [17] B. Aubert *et al.* [BaBar Collaboration], Phys. Rev. Lett. **90** (2003) 242001 [hep-ex/0304021].
 - [18] D. Besson *et al.* [CLEO Collaboration], Phys. Rev. D **68**, 032002 (2003) [Erratum-ibid. D **75**, 119908 (2007)] [hep-ex/0305100].
 - [19] E. V. Shuryak and I. Zahed, Phys. Rev. D **62**, 085014 (2000) [hep-ph/0005152].
 - [20] Y. Liu and I. Zahed, arXiv:1407.0384 [hep-ph].
 - [21] E. Shuryak and I. Zahed, Phys. Rev. D **89**, 094001 (2014) [arXiv:1311.0836 [hep-ph]].
 - [22] T. Kalaydzhyan and E. Shuryak, Phys. Rev. C **90**, 014901 (2014) [arXiv:1404.1888 [hep-ph]].